

# Recurrence coefficients for the semiclassical Laguerre weight and d-P $(A_2^{(1)}/E_6^{(1)})$ equations

**Siqi Chen**

School of Mathematics and Statistics, Qilu University of Technology (Shandong Academy of Sciences)  
Jinan 250353, China  
E-mail: [chen\\_siqi0301@163.com](mailto:chen_siqi0301@163.com)

**Mengkun Zhu**

School of Mathematics and Statistics, Qilu University of Technology (Shandong Academy of Sciences)  
Jinan 250353, China  
E-mail: [zmk@qlu.edu.cn](mailto:zmk@qlu.edu.cn)

*Keywords:* Orthogonal polynomials, Painlevé equations, Birational transformations

*MSC2020:* 33C47, 34M55, 14E07

## Abstract

In this paper, we use Sakai's geometric framework to explore the profound interconnection between recurrence coefficients of the semiclassical Laguerre weight  $w(x) = x^\lambda e^{-x^2+sx}$ ,  $x \in \mathbb{R}^+$ ,  $\lambda > -1$ ,  $s \in \mathbb{R}$ , and Painlevé equations. Specifically, we introduce a new transformation for the expressions obtained by Filipuk et al. in their analysis of ladder operators for semiclassical Laguerre polynomials, thereby deriving a recurrence relation. Subsequently, we establish a correspondence between this recurrence relation and a class of d-P  $(A_2^{(1)}/E_6^{(1)})$  equations.

## 1 Introduction

Orthogonal polynomials play a fundamental role in various branches of mathematics and mathematical physics, including random matrix theory, approximation theory, numerical analysis, and so on. In recent years, the relationship between recurrence coefficients of semiclassical orthogonal polynomials and solutions to discrete or differential Painlevé equations has attracted significant attention. For example, Magnus [Mag95] studied the weight function

$$w(x) = e^{x^3/3+sx}, \quad x^3 < 0, \quad s \in \mathbb{R},$$

and established a connection between the recurrence coefficients and the P<sub>II</sub> equation. In [CI10], Chen and Its investigated the singularly perturbed Laguerre weight

$$w(x) = x^\lambda e^{-x-s/x}, \quad x \geq 0, \quad \lambda \in \mathbb{R}^+, \quad s \in \mathbb{R}^+.$$

Their findings revealed that the diagonal recurrence coefficient of monic orthogonal polynomials satisfies a particular P<sub>III'</sub> equation. Clarkson and Jordaan [CJ14] showed that the recurrence coefficients of the semiclassical Laguerre weight

$$w(x) := w(x; s) = x^\lambda e^{-x^2+sx}, \quad x \in \mathbb{R}^+, \quad \lambda > -1, \quad s \in \mathbb{R}, \tag{1.1}$$

satisfy differential equations that are related to P<sub>IV</sub> equation. See also [BVA10, CJK16, FVAZ12, VA18].

In [Sak01], Sakai proposed a classification scheme for both continuous and discrete Painlevé equations, based on the geometric theory of Painlevé equations. He gave a complete classification of all possible configuration spaces for discrete Painlevé dynamics, demonstrating that each such configuration space is a family of specific rational algebraic surfaces, known as generalized Halphen surfaces.

In this paper, based on Sakai's work, we also focus on the semiclassical Laguerre weight (1.1), while another semiclassical Laguerre weight  $w(x) = x^\lambda e^{-N(x+c(x^2-x))}$  is discussed in [DFS22]. Consider a sequence of monic polynomials  $P_n(x; s) = x^n + \mathbf{p}(n, s)x^{n-1} + \dots$  orthogonal with respect to the weight (1.1), i.e.,

$$\int_0^\infty P_j(x; s)P_k(x; s)x^\lambda e^{-x^2+sx}dx = \delta_{j,k}h_j(s),$$

where  $h_j(s)$  denotes the  $L^2$ -norm of squared of  $P_j(x; s)$ . These monic orthogonal polynomials satisfy the three-term recurrence relation

$$xP_n(x; s) = P_{n+1}(x; s) + \alpha_n(s)P_n(x; s) + \beta_n(s)P_{n-1}(x; s),$$

with the initial condition  $P_0(x; s) = 1$ ,  $P_{-1}(x; s) = 0$ .

In [BVA10], it was shown that the recurrence coefficients satisfy the discrete system

$$\begin{cases} \tilde{x}_{n-1}\tilde{x}_n = \frac{\tilde{y}_n + n + \frac{1}{2}\lambda}{\tilde{y}_n^2 - \frac{1}{4}\lambda^2}, \\ \tilde{y}_n + \tilde{y}_{n+1} = \frac{1}{\tilde{x}_n} \left( \frac{s}{\sqrt{2}} - \frac{1}{\tilde{x}_n} \right), \end{cases} \quad (1.2)$$

where

$$\tilde{x}_n(s) = \frac{\sqrt{2}}{s - 2\alpha_n(s)}, \quad \tilde{y}_n(s) = 2\beta_n(s) - n - \frac{1}{2}\lambda,$$

and the system (1.2) can be derived from an asymmetric d-P<sub>IV</sub> equation via a limiting process.

Another way to studying the recurrence coefficients of orthogonal polynomials  $P_n(x; s)$  is to use

$$\begin{aligned} \left( \frac{d}{dx} + B_n(x; s) \right) P_n(x; s) &= \beta_n(s)A_n(x; s)P_{n-1}(x; s), && \text{lowering operator} \\ \left( \frac{d}{dx} - B_n(x; s) - v'(x) \right) P_{n-1}(x; s) &= -A_{n-1}(x; s)P_n(x; s), && \text{raising operator} \end{aligned}$$

where  $A_n(x; s)$  and  $B_n(x; s)$  are parameterized by the functions  $R_n(s)$  and  $r_n(s)$ ,

$$xA_n(x; s) = 2x + R_n(s), \quad xB_n(x; s) = r_n(s), \quad (1.3)$$

here,

$$\begin{aligned} R_n(s) &= \frac{\lambda}{h_n(s)} \int_0^\infty P_n^2(y; s)y^{\lambda-1}e^{-y^2+sy}dy, \\ r_n(s) &= \frac{\lambda}{h_{n-1}(s)} \int_0^\infty P_n(y; s)P_{n-1}(y; s)y^{\lambda-1}e^{-y^2+sy}dy. \end{aligned}$$

The functions  $A_n(x)$  and  $B_n(x)$  also satisfy the following modified compatibility conditions,

$$B_{n+1}(x) + B_n(x) = (x - \alpha_n(s))A_n(x) - v'(x), \quad (S_1)$$

$$1 + (x - \alpha_n(s))(B_{n+1}(x) - B_n(x)) = \beta_{n+1}(s)A_{n+1}(x) - \beta_n(s)A_{n-1}(x), \quad (S_2)$$

$$B_n^2(x) + v'(x)B_n(x) + \sum_{j=0}^{n-1} A_j(x) = \beta_n(s)A_n(x)A_{n-1}(x), \quad (S'_2)$$

where  $v(x) = -\ln w(x)$ . In [FVAZ12], Filipuk et al. obtained the following by substituting equation (1.3) into (S<sub>1</sub>) and (S'<sub>2</sub>) and comparing the coefficients of the same powers of  $x$ ,

$$R_n(s) = 2\alpha_n(s) - s, \quad (1.4)$$

$$r_n(s) + r_{n-1}(s) = \lambda - \alpha_n(s)R_n(s), \quad (1.5)$$

$$r_n(s) = 2\beta_n(s) - n, \quad (1.6)$$

$$r_n^2(s) - \lambda r_n(s) = \beta_n(s)R_{n-1}(s)R_n(s), \quad (1.7)$$

where (1.4)-(1.7) correspond to (21), (22), (25) and (27) in [FVAZ12].

According to (1.4)-(1.7), we introduce a new different transformation  $x_n(s)$ ,  $y_n(s)$  via

$$x_n(s) := \frac{1}{R_{n-1}(s)}, \quad y_n(s) := -r_n(s),$$

which yields

$$\begin{cases} x_n x_{n+1} = \frac{n - y_n}{2y_n^2 + 2\lambda y_n}, \\ y_n + y_{n-1} = -\frac{2\lambda x_n^2 - sx_n - 1}{2x_n^2}. \end{cases} \quad (1.8)$$

This recurrence relation mirrors the structure of (25) in [GR14], known to generate discrete Painlevé equations. By systematically applying the reduction methodology outlined in [DFS20], we demonstrate that this recurrence relation (1.8) is a discrete Painlevé equation that is equivalent to the standard example in the d-P  $(A_2^{(1)}/E_6^{(1)})$  family. Our main result is as follows.

**Theorem 1.** *The recurrence (1.8) is equivalent to the standard discrete Painlevé equation (2.11)*

$$\bar{q} + q = p - t - \frac{a_2}{p}, \quad p + \underline{p} = q + t + \frac{a_1}{q},$$

written in [KNY17]. This equivalence is achieved via the following change of variables:

$$x(q, p) = \frac{q}{\sqrt{2}(a_1 - qp)}, \quad y(q, p) = qp - a_1, \quad s(t) = \sqrt{2}t. \quad (1.9)$$

The inverse change of variables is given by

$$q(x, y) = -\sqrt{2}xy, \quad p(x, y) = \frac{n - y}{\sqrt{2}xy}, \quad t(s) = \frac{s}{\sqrt{2}}. \quad (1.10)$$

The relationship between the semiclassical Laguerre weight recurrence parameters and the root variables of discrete Painlevé equations is given by

$$a_0 = 1 - \lambda, \quad a_1 = -n, \quad a_2 = n + \lambda. \quad (1.11)$$

## 2 Discrete Painlevé Equations in the d-P $(A_2^{(1)}/E_6^{(1)})$ family

In this section, to ensure the self-contained nature of this paper, we have summarized the fundamental facts about the geometry of the  $E_6^{(1)}$ -family of Sakai surfaces and the standard discrete Painlevé equation associated with this surface family. For the standard example, we use  $(q, p)$ -coordinates and adopt the standard surface root basis illustrated in Figure 1 and the standard symmetry root basis shown in Figure 2, as outlined in the reference [KNY17].

### 2.1 The Point Configuration

The Picard lattice of a rational algebraic surface  $\mathcal{X}$ , which is obtained by blowing up eight points on  $\mathbb{P}^1 \times \mathbb{P}^1$ , is generated by the following classes,

$$\text{Pic}(\mathcal{X}) = \text{Span}_{\mathbb{Z}}\{\mathcal{H}_q, \mathcal{H}_p, \mathcal{E}_1, \dots, \mathcal{E}_8\},$$

and this lattice is equipped with the symmetric bilinear product (the intersection form), which is defined on the generators by  $\mathcal{H}_q \bullet \mathcal{H}_q = \mathcal{H}_p \bullet \mathcal{H}_p = \mathcal{H}_q \bullet \mathcal{E}_i = \mathcal{H}_p \bullet \mathcal{E}_j = 0$ ,  $\mathcal{H}_q \bullet \mathcal{H}_p = 1$ , and  $\mathcal{E}_i \bullet \mathcal{E}_j = -\delta_{ij}$ . Within this

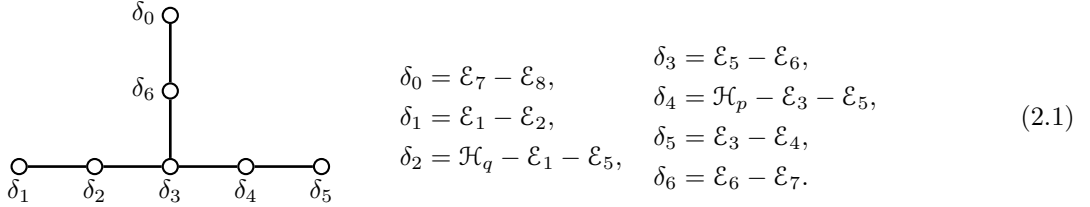


Figure 1: The standard surface root basis for the  $E_6^{(1)}$  surface sub-lattice.

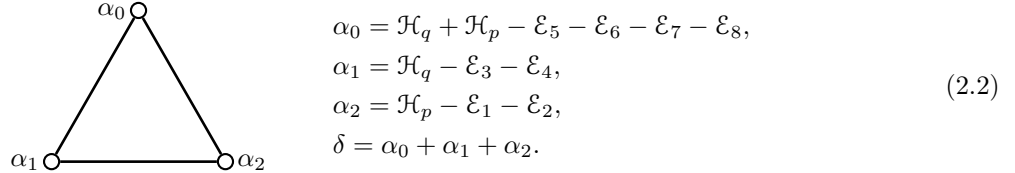


Figure 2: The standard symmetry root basis for the  $A_2^{(1)}$  symmetry sub-lattice.

lattice, the anti-canonical divisor class is given by  $-\mathcal{K}_{\mathcal{X}} = 2\mathcal{H}_q + 2\mathcal{H}_p - \mathcal{E}_1 - \mathcal{E}_2 - \mathcal{E}_3 - \mathcal{E}_4 - \mathcal{E}_5 - \mathcal{E}_6 - \mathcal{E}_7 - \mathcal{E}_8$ . For the  $E_6^{(1)}$  surface, this class should decompose into irreducible components each with self-intersection  $-2$ , specifically as

$$-\mathcal{K}_{\mathcal{X}} = \delta = \delta_0 + \delta_1 + 2\delta_2 + 3\delta_3 + 2\delta_4 + \delta_5 + 2\delta_6,$$

and this decomposition is given by the choice of the surface root basis shown on Figure 1.

We now proceed to describe the corresponding point configuration. Let  $Q = 1/q$  and  $P = 1/p$  denote the coordinates at infinity. By using the Möbius group action, we can arrange the points to be  $p_1(\infty, 0)$ ,  $p_3(0, \infty)$ ,  $p_5(\infty, \infty)$ , and the only remaining gauge action is the rescaling of the  $q$ -coordinate (to be utilized later for normalizing the root variables). We then get the point configuration shown on Figure 3. It is worth noting that one reason for adopting this point normalization is that they are located on the polar divisor of the standard symplectic form  $\omega = dq \wedge dp$ .

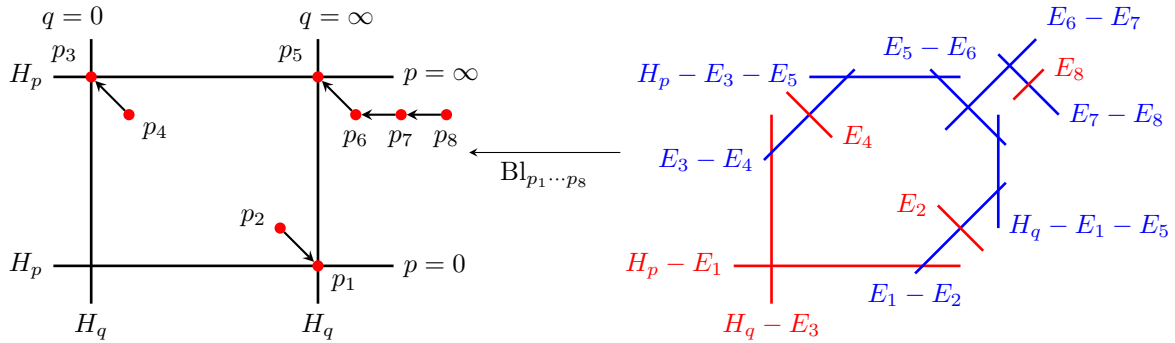


Figure 3: The model Sakai surface for the d-P  $(A_2^{(1)}/E_6^{(1)})$  example.

The parameterization of this point configuration in terms of root variables  $a_0, a_1, a_2$  normalized by  $a_0 + a_1 + a_2 = 1$  is given in [KNY17],

$$p_{12} \left( \frac{1}{\varepsilon}, -a_2 \varepsilon \right)_2, \quad p_{34} \left( a_1 \varepsilon, \frac{1}{\varepsilon} \right)_2, \quad p_{5678} \left( \frac{1}{\varepsilon}, \frac{1}{\varepsilon} + t + (a_1 + a_2 - 1) \varepsilon \right)_4,$$

or, explicitly,

$$\begin{aligned}
p_1 \left( Q = \frac{1}{q} = 0, p = 0 \right) &\quad \leftarrow p_2 \left( u_1 = \frac{1}{q} = 0, v_1 = qp = -a_2 \right), \\
p_3 \left( q = 0, P = \frac{1}{p} = 0 \right) &\quad \leftarrow p_4 \left( U_3 = qp = a_1, V_3 = \frac{1}{p} = 0 \right), \\
p_5 \left( Q = \frac{1}{q} = 0, P = \frac{1}{p} = 0 \right) &\leftarrow p_6 \left( u_5 = \frac{1}{q} = 0, v_5 = \frac{q}{p} = 1 \right) \\
&\quad \leftarrow p_7 \left( u_6 = \frac{1}{q} = 0, v_6 = \frac{q^2 - qp}{p} = -t \right) \\
&\quad \leftarrow p_8 \left( u_7 = \frac{1}{q} = 0, v_7 = \frac{q^3 - q^2 p + tqp}{p} = t^2 + a_0 \right).
\end{aligned} \tag{2.3}$$

## 2.2 The Extended Affine Weyl Symmetry Group

Recall that, the algebraic source of Painlevé dynamics stems from the birational representation of the extended affine Weyl symmetry group  $\widetilde{W}(A_2^{(1)}) = \text{Aut}(A_2^{(1)}) \ltimes W(A_2^{(1)})$ .

The affine Weyl group  $W(A_2^{(1)})$  is defined via generators  $w_i = w_{\alpha_i}$  and relations that are encoded in the diagram on Figure 2,

$$W(A_2^{(1)}) = W \left( \begin{array}{c} \alpha_0 \\ \triangle \\ \alpha_1 \quad \alpha_2 \end{array} \right) = \left\langle w_0, w_1, w_2 \mid \begin{array}{ll} w_i^2 = e, & w_i \circ w_j = w_j \circ w_i \quad \text{when } \begin{array}{c} \bullet \\ \alpha_i \end{array} \begin{array}{c} \bullet \\ \alpha_j \end{array} \\ w_i \circ w_j \circ w_i = w_j \circ w_i \circ w_j \quad \text{when } \begin{array}{c} \bullet \\ \alpha_i \end{array} \begin{array}{c} \bullet \\ \alpha_j \end{array} \end{array} \right\rangle.$$

In our setting, this group is represented by actions on  $\text{Pic}(\mathcal{X})$  induced by reflections in the roots  $\alpha_i$ ,

$$w_i(\mathcal{C}) = w_{\alpha_i}(\mathcal{C}) = \mathcal{C} - 2 \frac{\mathcal{C} \bullet \alpha_i}{\alpha_i \bullet \alpha_i} \alpha_i = \mathcal{C} + (\mathcal{C} \bullet \alpha_i) \alpha_i, \quad \mathcal{C} \in \text{Pic}(\mathcal{X}). \tag{2.4}$$

Next, we need to extend this group by the Dynkin diagram automorphism group  $\text{Aut}(A_2^{(1)})$ , which is isomorphic to the dihedral group  $\mathbb{D}_3$  (the symmetry group of a triangle). This group is generated by two reflections (here we use the standard cycle notations for permutations),

$$\sigma_1 = (\alpha_1 \alpha_2) = (\delta_1 \delta_5)(\delta_2 \delta_4), \quad \sigma_2 = (\alpha_0 \alpha_2) = (\delta_0 \delta_1)(\delta_2 \delta_6). \tag{2.5}$$

Then  $\sigma_i$  act on the  $\text{Pic}(\mathcal{X})$  as

$$\sigma_1 = w_{\mathcal{E}_1 - \mathcal{E}_3} \circ w_{\mathcal{E}_2 - \mathcal{E}_4} \circ w_{\mathcal{H}_q - \mathcal{H}_p}, \quad \sigma_2 = w_{\mathcal{E}_1 - \mathcal{E}_7} \circ w_{\mathcal{E}_2 - \mathcal{E}_8} \circ w_{\mathcal{H}_q - \mathcal{E}_5 - \mathcal{E}_6}.$$

**Lemma 2.** [TD25] *The generators of the extended affine Weyl group  $\widetilde{W}(A_2^{(1)})$  act to transform an initial point configuration*

$$\left( a_0, \quad a_1, \quad a_2 ; \quad t ; \frac{q}{p} \right)$$

as follows:

$$w_0 : \left( a_0, a_1, a_2 ; t ; \frac{q}{p} \right) \mapsto \left( -a_0, a_1 + a_0, a_2 + a_0 ; t ; \frac{q - \frac{a_0}{q-p+t}}{p - \frac{a_0}{q-p+t}} \right), \quad (2.6)$$

$$w_1 : \left( a_0, a_1, a_2 ; t ; \frac{q}{p} \right) \mapsto \left( a_0 + a_1, -a_1, a_2 + a_1 ; t ; \frac{q}{p - \frac{a_1}{q}} \right), \quad (2.7)$$

$$w_2 : \left( a_0, a_1, a_2 ; t ; \frac{q}{p} \right) \mapsto \left( a_0 + a_2, a_1 + a_2, -a_2 ; t ; \frac{q + \frac{a_2}{p}}{p} \right), \quad (2.8)$$

$$\sigma_1 : \left( a_0, a_1, a_2 ; t ; \frac{q}{p} \right) \mapsto \left( -a_0, -a_2, -a_1 ; t ; \frac{-p}{-q} \right), \quad (2.9)$$

$$\sigma_2 : \left( a_0, a_1, a_2 ; t ; \frac{q}{p} \right) \mapsto \left( -a_2, -a_1, -a_0 ; t ; \frac{q}{q - p + t} \right). \quad (2.10)$$

*Proof.* This proof is standard, for details, refer to [DFS20] and [DT18]. Here, we only briefly outline the computation of (2.7). The reflection  $w_1$  in the root  $\alpha_1 = \mathcal{H}_q - \mathcal{E}_3 - \mathcal{E}_4$  acts on the  $\text{Pic}(\mathcal{X})$  by

$$w_1(\mathcal{H}_q) = \mathcal{H}_q, \quad w_1(\mathcal{H}_p) = \mathcal{H}_q + \mathcal{H}_p - \mathcal{E}_3 - \mathcal{E}_4,$$

and

$$w_1(\mathcal{E}_3) = \mathcal{H}_q - \mathcal{E}_4, \quad w_1(\mathcal{E}_4) = \mathcal{H}_q - \mathcal{E}_3, \quad w_1(\mathcal{E}_i) = \mathcal{E}_i, \quad i = 1, 2, 5, 6, 7, 8.$$

Thus, we are looking for a mapping  $w_1$  which, in the affine chart  $(q, p)$ , is defined by a formula  $w_1(q, p) = (\bar{q}, \bar{p})$ , so that

$$w_1^*(\mathcal{H}_{\bar{q}}) = \mathcal{H}_q, \quad w_1^*(\mathcal{H}_{\bar{p}}) = \mathcal{H}_q + \mathcal{H}_p - \mathcal{E}_3 - \mathcal{E}_4.$$

Hence, up to Möbius transformations,  $\bar{q}$  coincides with  $q$ , and  $\bar{p}$  is a coordinate on a pencil of  $(1, 1)$ -curves passing through the degeneration cascade  $p_3(0, \infty) \leftarrow p_4(U_3 = a_1, V_3 = 0)$ , then

$$|H_{\bar{p}}| = \{Aqp + Bq + Cp + D = 0\} = \{A(qp - a_1) + Bq = 0\}.$$

Considering Möbius transformations, we obtain

$$\bar{q} = \frac{Aq + B}{Cq + D}, \quad \bar{p} = \frac{Kq + L(qp - a_1)}{Mq + N(qp - a_1)},$$

where  $A, \dots, N$  are constants to be determined. We can also get the root variables change as  $\bar{a}_0 = a_0 + a_1$ ,  $\bar{a}_1 = -a_1$  and  $\bar{a}_2 = a_2 + a_1$ .

Since  $w_1(\mathcal{E}_1 - \mathcal{E}_2) = \mathcal{E}_1 - \mathcal{E}_2$ ,  $(\bar{q}, \bar{p})(\infty, 0) = (\infty, 0)$ , we find that  $C = 0$ ,  $K = 0$ ,  $D = 1$  and  $L = 1$ . Similarly, from  $w_1(\mathcal{E}_3 - \mathcal{E}_4) = \mathcal{E}_3 - \mathcal{E}_4$ , it follows that  $(\bar{q}, \bar{p})(0, \infty) = (0, \infty)$ , hence  $B = 0$ . From  $w_1(\mathcal{E}_5 - \mathcal{E}_6) = \mathcal{E}_5 - \mathcal{E}_6$ , we further find that  $(\bar{q}, \bar{p})(\infty, \infty) = (\infty, \infty)$ , so  $N = 0$ . Thus,

$$\bar{q} = Aq, \quad \bar{p} = \frac{qp - a_1}{Mq},$$

from  $w_1(\mathcal{E}_2) = \mathcal{E}_2$ , we derive  $\frac{A}{M} = 1$ , from  $w_1(\mathcal{E}_6 - \mathcal{E}_7) = \mathcal{E}_6 - \mathcal{E}_7$ , we get  $AM = 1$ . Finally, from  $w_1(\mathcal{E}_7 - \mathcal{E}_8) = \mathcal{E}_7 - \mathcal{E}_8$ , we obtain  $A = M = 1$ .  $\square$

### 2.3 Discrete Painlevé equations on the $E_6^{(1)}$ surface

In [KNY17], the standard example of a discrete Painlevé equation on the  $E_6^{(1)}$ -surface is given in Section 8.1.18 equation (8.25) as

$$\bar{q} + q = p - t - \frac{a_2}{p}, \quad p + \underline{p} = q + t + \frac{a_1}{q}, \quad (2.11)$$

with the root variables evolution and normalization as follows

$$\bar{a}_0 = a_0, \quad \bar{a}_1 = a_1 - 1, \quad \bar{a}_2 = a_2 + 1, \quad a_0 + a_1 + a_2 = 1. \quad (2.12)$$

From the evolution of the root variables (2.12) we can immediately see that the corresponding translation on the root lattice is

$$\varphi_* : \alpha = \langle \alpha_0, \alpha_1, \alpha_2 \rangle \mapsto \varphi_*(\alpha) = \alpha + \langle 0, 1, -1 \rangle \delta. \quad (2.13)$$

Using the standard techniques, see [DT18] for a detailed example, we get the following decomposition of  $\varphi$  in terms of the generators of  $\widetilde{W}(A_2^{(1)})$ :

$$\varphi = \sigma_1 \sigma_2 w_0 w_2. \quad (2.14)$$

*Remark 3.* With the following relabeling of the root basis,

$$b_0 = a_2, \quad b_2 = a_1, \quad b_1 = a_0,$$

and the substitutions

$$f = -q, \quad g = p,$$

equation (2.11) is found to coincide with equations (2.39)-(2.40) in [Sak07], i.e.

$$f + \bar{f} = t - g + \frac{b_0}{g}, \quad g + \bar{g} = t - \bar{f} - \frac{b_2 - 1}{\bar{f}}. \quad (2.15)$$

This system of equations is referred to as the d-P<sub>II</sub> equation in Section 7 of [Sak01].

### 3 The Identification Procedure

In this Section, we follow the reduction procedures introduced in [DFS20] to establish the correspondence between the recurrence relation (1.8) and the standard example (2.11).

#### 3.1 The Singularity Structure

In the geometric analysis of discrete Painlevé equations, the first step is to understand the singularity structure of the system. The recurrence relation (1.8) induces two fundamental mappings, the *forward mapping*  $\psi_1^{(n)} : (x_n, y_n) \mapsto (x_{n+1}, y_n)$  and the *backward mapping*  $\psi_2^{(n)} : (x_n, y_n) \mapsto (x_n, y_{n-1})$ . In this paper, we focus on the composed mapping  $\psi^{(n)} = (\psi_2^{(n+1)})^{-1} \circ \psi_1^{(n)} : (x_n, y_n) \mapsto (x_{n+1}, y_{n+1})$ . We put  $x := x_n$ ,  $\bar{x} := x_{n+1}$ ,  $y := y_n$ ,  $\bar{y} := y_{n+1}$  and omit the index  $n$  in the mapping notation. The map  $\psi : (x, y) \mapsto (\bar{x}, \bar{y})$  then becomes

$$\begin{cases} \bar{x} = \frac{n - y}{2xy(y + \lambda)}, \\ \bar{y} = -\frac{(y + \lambda)(n^2 - n(2 + sx)y + (1 + sx - 2\lambda x^2)y^2 - 2x^2y^3)}{(y - n)^2}. \end{cases} \quad (3.1)$$

To compactify the affine complex plane  $\mathbb{C} \times \mathbb{C}$  into  $\mathbb{P}^1 \times \mathbb{P}^1$ , we introduce three supplementary coordinate charts  $(X, y)$ ,  $(x, Y)$  and  $(X, Y)$ , where  $X = 1/x$ ,  $Y = 1/y$ . By examining the coordinate where both the numerator and the denominator of the mapping vanish, we immediately see the following base points,

$$q_1(0, n), \quad q_2(\infty, -\lambda), \quad q_3(\infty, 0), \quad q_4(0, \infty).$$

At each of these base points, we perform the blowup procedure, see, e.g., [Sha13], which entails introducing two new local coordinate charts,  $(u_i, v_i)$  and  $(U_i, V_i)$ , in the neighborhood of the base point  $q_i(x_i, y_i)$ . The variable transformations are defined as

$$x = x_i + u_i = x_i + U_i V_i, \quad y = y_i + u_i v_i = y_i + V_i.$$

The coordinates  $v_i = 1/U_i$  parameterize all possible slopes of lines through  $q_i$ , and so this variable change ‘separates’ all curves passing through  $q_i$  based on their slopes. The blowup procedure induces a bijection on the punctured neighborhood of  $q_i$ , replacing  $q_i$  with a projective line  $\mathbb{P}^1$  (*exceptional divisor*  $F_i$ ), locally defined by  $u_i = 0$  and  $V_i = 0$  in the blowup charts. Extending the mapping to these charts via coordinate substitutions may reveal new base points on  $F_i$  (where  $u_i = V_i = 0$ ). For discrete Painlevé case, iterative blowups finitely resolve all base points, then the following lemma is established.

**Lemma 4.** *The base points of the mapping (3.1) are*

$$\begin{aligned} q_1(x=0, y=n), \\ q_2\left(X=\frac{1}{x}=0, y=-\lambda\right), \quad q_3\left(X=\frac{1}{x}=0, y=0\right), \\ q_4\left(x=0, Y=\frac{1}{y}=0\right) \leftarrow q_5\left(u_4=x=0, v_4=\frac{1}{xy}=0\right) \\ \leftarrow q_6\left(u_5=x=0, v_5=\frac{1}{x^2y}=2\right) \\ \leftarrow q_7\left(u_6=x=0, v_6=\frac{1-2x^2y}{x^3y}=-2s\right) \\ \leftarrow q_8\left(u_7=x=0, v_7=\frac{1-2x^2y+2sx^3y}{x^4y}=2(s^2+2(n+\lambda-1))\right). \end{aligned} \tag{3.2}$$

Considering the inverse mapping does not add any new base points.

After the blowup of all eight base points  $q_i$ , we obtain a (family of) rational algebraic surfaces parameterized by  $\lambda$ ,  $s$  and  $n$  (the coordinates of the base points), denoted as  $\mathcal{X} = \mathcal{X}_{\mathbf{b}}$  with  $\mathbf{b} = \{\lambda, s, n\}$ .

### 3.2 The Induced Mapping on $\text{Pic}(\mathcal{X})$

In the identification procedure, the next step involves computing the induced mapping on the Picard lattice. For the product space  $\mathbb{P}^1 \times \mathbb{P}^1$ , its Picard lattice is generated by the linear equivalence classes of the coordinate lines. Specifically, we have  $\text{Pic}(\mathbb{P}^1 \times \mathbb{P}^1) = \text{Span}_{\mathbb{Z}}\{\mathcal{H}_x, \mathcal{H}_y\}$ , where  $\mathcal{H}_x = [H_{x=a}]$  denotes the class of a *vertical* line and  $\mathcal{H}_y = [H_{y=b}]$  denotes the class of a *horizontal* line on  $\mathbb{P}^1 \times \mathbb{P}^1$ . Each blowup procedure at a base point  $q_i$  adds the class  $\mathcal{F}_i = [F_i]$  of the *exceptional divisor* of the blowup, expanding the Picard lattice to

$$\text{Pic}(\mathcal{X}) = \text{Span}_{\mathbb{Z}}\{\mathcal{H}_x, \mathcal{H}_y, \mathcal{F}_1, \dots, \mathcal{F}_8\}.$$

$\text{Pic}(\mathcal{X})$  is equipped with the symmetric bilinear *intersection form* given by

$$\mathcal{H}_x \bullet \mathcal{H}_x = \mathcal{H}_y \bullet \mathcal{H}_y = \mathcal{H}_x \bullet \mathcal{F}_i = \mathcal{H}_y \bullet \mathcal{F}_j = 0, \quad \mathcal{H}_x \bullet \mathcal{H}_y = 1, \quad \mathcal{F}_i \bullet \mathcal{F}_j = -\delta_{ij} \tag{3.3}$$

on the generators, and then extended by the linearity.

The mapping  $\psi$  induces a linear map on  $\text{Pic}(\mathcal{X})$ , note that  $\text{Pic}(\mathcal{X})$  and  $\text{Pic}(\bar{\mathcal{X}})$  are clearly canonically isomorphic, so we often use the notation  $\text{Pic}(\mathcal{X})$ . We denote by  $\bar{F}_i$  the class of the exceptional divisor obtained by the blowup at  $\bar{q}_i = \psi(q_i)$  and use the notation  $\mathcal{F}_{i \dots j} = \mathcal{F}_i + \dots + \mathcal{F}_j$ . This computation follows standard computation detailed in [DT18, DFS20], so we only summarize the result here.

**Lemma 5.** *The action of the mapping  $\psi_* : \text{Pic}(\mathcal{X}) \rightarrow \text{Pic}(\bar{\mathcal{X}})$  is given by*

$$\begin{aligned} \mathcal{H}_x &\mapsto 4\bar{\mathcal{H}}_x + 2\bar{\mathcal{H}}_y - \bar{F}_{23} - 2\bar{F}_{456} - \bar{F}_{78}, & \mathcal{H}_y &\mapsto 2\bar{\mathcal{H}}_x + \bar{\mathcal{H}}_y - \bar{F}_{4567}, \\ \mathcal{F}_1 &\mapsto 2\bar{\mathcal{H}}_x + \bar{\mathcal{H}}_y - \bar{F}_{45678}, & \mathcal{F}_5 &\mapsto \bar{\mathcal{H}}_x - \bar{F}_6, \\ \mathcal{F}_2 &\mapsto 2\bar{\mathcal{H}}_x + \bar{\mathcal{H}}_y - \bar{F}_{34567}, & \mathcal{F}_6 &\mapsto \bar{\mathcal{H}}_x - \bar{F}_5, \\ \mathcal{F}_3 &\mapsto 2\bar{\mathcal{H}}_x + \bar{\mathcal{H}}_y - \bar{F}_{24567}, & \mathcal{F}_7 &\mapsto \bar{\mathcal{H}}_x - \bar{F}_4, \\ \mathcal{F}_4 &\mapsto \bar{\mathcal{H}}_x + \bar{\mathcal{H}}_y - \bar{F}_{456}, & \mathcal{F}_8 &\mapsto \bar{F}_1. \end{aligned}$$

The evolution of parameters (and hence, the base points) is given by  $\mathbf{b} = \{\lambda, s, n\} \mapsto \bar{\mathbf{b}} = \{\lambda, s, n+1\}$ .

### 3.3 The Surface Type

Given that the mapping is fully regularized via eight blowups, it naturally fits into the discrete Painlevé equations framework. To determine the algebraic surface type, we analyze the configuration of irreducible components of the bi-degree  $(2, 2)$  curve  $\Gamma$  that contains the base points  $q_1, \dots, q_8$  of the mapping. For generic parameters, the proper transform of  $\Gamma$  under these blowups is the unique *anti-canonical divisor*  $-K_X$ , which corresponds to the polar divisor of a symplectic form  $\omega$  and serves as a critical invariant for algebraic surface classification. The projection mapping

$$\eta : \mathcal{X}_b = \text{Bl}_{q_1 \dots q_8}(\mathbb{P}^1 \times \mathbb{P}^1) \rightarrow \mathbb{P}^1 \times \mathbb{P}^1,$$

formally establishes the birational equivalence between the singular initial space and the regularized blown-up surface  $\mathcal{X}_b$ , where the eight blowups resolve base-point singularities to embed the mapping within the discrete Painlevé framework.

**Lemma 6.** *The base points  $q_1, \dots, q_8$  of the mapping (3.1) are situated on the bi-quadratic curve  $\Gamma$ , which is defined in the affine chart by the equation  $x = 0$ . The homogeneous equation of  $\Gamma$  is  $x^0 x^1 (y^1)^2 = 0$ , where  $x = x^0/x^1$  and  $y = y^0/y^1$ , confirming that  $\Gamma$  is indeed a bi-quadratic curve. It is important to note that certain points exhibit infinitely-close degeneration cascades. The irreducible components  $d_i$  of the proper transform  $-K_X$  of  $\Gamma$ ,*

$$-K_X = 2H_x + 2H_y - F_1 - \dots - F_8 = d_0 + d_1 + 2d_2 + 3d_3 + 2d_4 + d_5 + 2d_6,$$

are given by

$$\begin{aligned} d_0 &= F_7 - F_8, & d_1 &= H_x - F_2 - F_3, & d_2 &= H_y - F_4 - F_5, & d_3 &= F_5 - F_6, \\ d_4 &= F_4 - F_5, & d_5 &= H_x - F_1 - F_4, & d_6 &= F_6 - F_7, \end{aligned} \quad (3.4)$$

they define the surface root basis  $\delta_1, \dots, \delta_6$  (where  $\delta_i = [d_i]$ ) of  $-2$ -classes in  $\text{Pic}(X)$  whose configuration is described by the Dynkin diagram of type  $E_6^{(1)}$ :

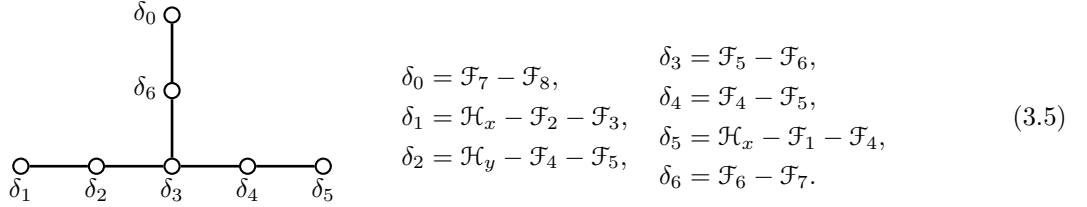


Figure 4: The surface root basis for the semiclassical Laguerre weight recurrence.

The generalized Cartan matrix of affine type  $E_6^{(1)}$  [Kac90] is

$$\delta_i \bullet \delta_j = \begin{pmatrix} -2 & 0 & 0 & 0 & 0 & 0 & 1 \\ 0 & -2 & 1 & 0 & 0 & 0 & 0 \\ 0 & 1 & -2 & 1 & 0 & 0 & 0 \\ 0 & 0 & 1 & -2 & 1 & 0 & 1 \\ 0 & 0 & 0 & 1 & -2 & 1 & 0 \\ 0 & 0 & 0 & 0 & 1 & -2 & 0 \\ 1 & 0 & 0 & 1 & 0 & 0 & -2 \end{pmatrix}. \quad (3.6)$$

In Figure 5, we display the final stage of the blowup process and the resulting  $E_6^{(1)}$  surface. Consequently, our recurrence relation is classified within the d-P  $(A_2^{(1)}/E_6^{(1)})$  family, characterized by the symmetry group

$\widetilde{W}(A_2^{(1)})$ . The details of the standard d-P  $(A_2^{(1)}/E_6^{(1)})$  point configuration, root bases for the surface, symmetry sub-lattices, and other relevant data are documented in Appendix, following the conventions established in [KNY17].

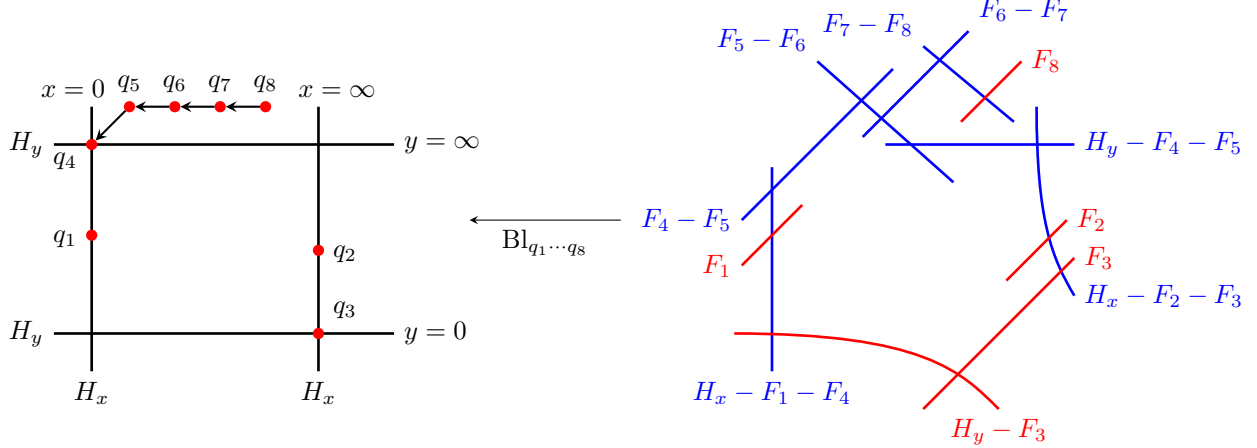


Figure 5: The Sakai surface for the semiclassical Laguerre weight recurrence.

### 3.4 Initial Geometry Identification

The next step in the identification procedure is to determine a basis transformation within  $\text{Pic}(\mathcal{X})$  from the basis  $\{\mathcal{H}_x, \mathcal{H}_y, \mathcal{F}_i\}$  to the basis  $\{\mathcal{H}_q, \mathcal{H}_p, \mathcal{E}_j\}$  that corresponds to the standard example. Here, we conduct an initial geometry matching, acknowledging that the resulting basis transformation is non-unique and may later require adjustment to match the dynamics.

**Lemma 7.** *The following change of basis of  $\text{Pic}(\mathcal{X})$  identifies the root bases between the standard  $E_6^{(1)}$  surface and the surface that we obtained for the semiclassical Laguerre weight recurrence:*

$$\begin{aligned}
\mathcal{H}_x &= \mathcal{H}_p, & \mathcal{H}_q &= \mathcal{H}_x + \mathcal{H}_y - \mathcal{F}_3 - \mathcal{F}_4, \\
\mathcal{H}_y &= \mathcal{H}_q + \mathcal{H}_p - \mathcal{E}_1 - \mathcal{E}_3, & \mathcal{H}_p &= \mathcal{H}_x, \\
\mathcal{F}_1 &= \mathcal{E}_4, & \mathcal{E}_1 &= \mathcal{H}_x - \mathcal{F}_3, \\
\mathcal{F}_2 &= \mathcal{E}_2, & \mathcal{E}_2 &= \mathcal{F}_2, \\
\mathcal{F}_3 &= \mathcal{H}_p - \mathcal{E}_1, & \mathcal{E}_3 &= \mathcal{H}_x - \mathcal{F}_4, \\
\mathcal{F}_4 &= \mathcal{H}_p - \mathcal{E}_3, & \mathcal{E}_4 &= \mathcal{F}_1, \\
\mathcal{F}_5 &= \mathcal{E}_5, & \mathcal{E}_5 &= \mathcal{F}_5, \\
\mathcal{F}_6 &= \mathcal{E}_6, & \mathcal{E}_6 &= \mathcal{F}_6, \\
\mathcal{F}_7 &= \mathcal{E}_7, & \mathcal{E}_7 &= \mathcal{F}_7, \\
\mathcal{F}_8 &= \mathcal{E}_8, & \mathcal{E}_8 &= \mathcal{F}_8.
\end{aligned}$$

*Proof.* This computation is straightforward and relies on comparing the surface root bases illustrated in Figure 4 and Figure 1.  $\square$

### 3.5 The Symmetry Roots and the Translations

We are now in the position to start comparing the dynamics. By starting with the standard selection of the symmetry root basis (2.2) and utilizing the basis transformation in Lemma 7, we derive the symmetry roots for the applied problem, as illustrated in Figure 6.

$$\begin{aligned}
\alpha_0 &= 2\mathcal{H}_x + \mathcal{H}_y - \mathcal{F}_3 - \mathcal{F}_4 - \mathcal{F}_5 - \mathcal{F}_6 - \mathcal{F}_7 - \mathcal{F}_8, \\
\alpha_1 &= \mathcal{H}_y - \mathcal{F}_1 - \mathcal{F}_3, \\
\alpha_2 &= \mathcal{F}_3 - \mathcal{F}_2, \\
\delta &= \alpha_0 + \alpha_1 + \alpha_2.
\end{aligned} \tag{3.7}$$

Figure 6: The symmetry root basis for the semiclassical Laguerre weight recurrence (preliminary choice).

From the action on  $\text{Pic}(\mathcal{X})$  specified in Lemma 5, we immediately deduce that the corresponding translation on the root lattice. We decompose  $\psi$  in terms of the generators of the extended affine Weyl symmetry group (see Section 2.2) and compare the results with the standard mapping  $\varphi$  given in Section 2.3. We obtain

$$\begin{aligned}
\psi_* : \alpha = \langle \alpha_0, \alpha_1, \alpha_2 \rangle &\mapsto \psi_*(\alpha) = \alpha + \langle 1, -1, 0 \rangle \delta, & \psi &= \sigma_1 \sigma_2 w_2 w_1, \\
\varphi_* : \alpha = \langle \alpha_0, \alpha_1, \alpha_2 \rangle &\mapsto \varphi_*(\alpha) = \alpha + \langle 0, 1, -1 \rangle \delta, & \varphi &= \sigma_1 \sigma_2 w_0 w_2.
\end{aligned}$$

We immediately observe that  $\psi = w_1 \circ \varphi \circ w_1^{-1}$  (note that  $w_1 \sigma_1 \sigma_2 = \sigma_1 \sigma_2 w_0$  and that  $w_1$  is an involution,  $w_1^{-1} = w_1$ ). Consequently, our dynamics are indeed equivalent to the standard equation (2.11), but the change of basis in Lemma 7 needs to be adjusted by acting by  $w_1$ . We do it in the next section.

### 3.6 Final Geometry Identification

**Lemma 8.** *After the change of basis of  $\text{Pic}(\mathcal{X})$  given by*

$$\begin{aligned}
\mathcal{H}_x &= \mathcal{H}_q + \mathcal{H}_p - \mathcal{E}_3 - \mathcal{E}_4, & \mathcal{H}_q &= \mathcal{H}_x + \mathcal{H}_y - \mathcal{F}_3 - \mathcal{F}_4, \\
\mathcal{H}_y &= \mathcal{H}_q + \mathcal{H}_p - \mathcal{E}_1 - \mathcal{E}_3, & \mathcal{H}_p &= \mathcal{H}_x + \mathcal{H}_y - \mathcal{F}_1 - \mathcal{F}_3, \\
\mathcal{F}_1 &= \mathcal{H}_q - \mathcal{E}_3, & \mathcal{E}_1 &= \mathcal{H}_x - \mathcal{F}_3, \\
\mathcal{F}_2 &= \mathcal{E}_2, & \mathcal{E}_2 &= \mathcal{F}_2, \\
\mathcal{F}_3 &= \mathcal{H}_q + \mathcal{H}_p - \mathcal{E}_1 - \mathcal{E}_3 - \mathcal{E}_4, & \mathcal{E}_3 &= \mathcal{H}_x + \mathcal{H}_y - \mathcal{F}_1 - \mathcal{F}_3 - \mathcal{F}_4, \\
\mathcal{F}_4 &= \mathcal{H}_p - \mathcal{E}_3, & \mathcal{E}_4 &= \mathcal{H}_y - \mathcal{F}_3, \\
\mathcal{F}_5 &= \mathcal{E}_5, & \mathcal{E}_5 &= \mathcal{F}_5, \\
\mathcal{F}_6 &= \mathcal{E}_6, & \mathcal{E}_6 &= \mathcal{F}_6, \\
\mathcal{F}_7 &= \mathcal{E}_7, & \mathcal{E}_7 &= \mathcal{F}_7, \\
\mathcal{F}_8 &= \mathcal{E}_8, & \mathcal{E}_8 &= \mathcal{F}_8.
\end{aligned}$$

the recurrence relations (1.8) for variables  $x_n$  and  $y_n$  coincides with the discrete Painlevé equation given by (2.11). The resulting identification of the symmetry root bases (the surface root bases do not change) is shown in Figure 7.

$$\begin{aligned}
\alpha_0 &= 2\mathcal{H}_x + 2\mathcal{H}_y - \mathcal{F}_1 - 2\mathcal{F}_3 - \mathcal{F}_4 - \mathcal{F}_5 - \mathcal{F}_6 - \mathcal{F}_7 - \mathcal{F}_8, \\
\alpha_1 &= -\mathcal{H}_y + \mathcal{F}_1 + \mathcal{F}_3, \\
\alpha_2 &= \mathcal{H}_y - \mathcal{F}_1 - \mathcal{F}_2, \\
\delta &= \alpha_0 + \alpha_1 + \alpha_2.
\end{aligned}$$

Figure 7: The symmetry root basis for the semiclassical Laguerre weight recurrence (final choice).

Next we need to realize this change of basis on  $\text{Pic}(\mathcal{X})$  by an explicit change of coordinates. For that, it is convenient to first match the parameters between the applied problem and the standard example. This is done with the help of the *Period Map*.

### 3.7 The Period Map and the Identification of Parameters

Before establishing the coordinate transformation that identifies the two dynamics, we need to match the semiclassical Laguerre weight parameters  $\lambda, s$  and the recurrence step  $n$  with the root variables  $a_i$ . These root variables are defined through the *Period Map*  $\mathcal{X} : Q \rightarrow \mathbb{C}$ , where  $a_i = \mathcal{X}(\alpha_i)$ . Additionally, it is readily observed that the points  $q_i$  lie on the polar divisor of a symplectic form, which in the affine  $(x, y)$ -chart is given by  $\omega = k \frac{dx \wedge dy}{x}$ . Consequently, the computation of the period map relies on the following results from [Sak01]:

- Each symmetry root  $\alpha_i$  can be represented (non-uniquely) as the difference of classes of two effective divisors,  $\alpha_i = [C_i^1] - [C_i^0]$ .
- For each such representation, there exists a unique irreducible component  $d_k$  of the anti-canonical divisor  $-K_{\mathcal{X}}$  satisfying  $d_k \bullet C_i^1 = d_k \bullet C_i^0 = 1$ . Define the intersection points  $P_i := d_k \cap C_i^0$  and  $Q_i := d_k \cap C_i^1$ .
- Consequently, the period map  $\mathcal{X}$  acts on  $\alpha_i$  as

$$\mathcal{X}(\alpha_i) = \mathcal{X}([C_i^1] - [C_i^0]) = \int_{P_i}^{Q_i} \frac{1}{2\pi i} \oint_{d_k} \omega = \int_{P_i}^{Q_i} \text{res}_{d_k} \omega. \quad (3.8)$$

Building on this, we establish the following lemma.

**Lemma 9.**

- (i) *The residues of the symplectic form  $\omega = k \frac{dx \wedge dy}{x}$  along the irreducible components of the polar divisor are given by*

$$\begin{aligned} \text{res}_{d_0} \omega &= -\frac{k}{4} dv_7, & \text{res}_{d_1} \omega &= -kdy, & \text{res}_{d_2} \omega &= 0, & \text{res}_{d_3} \omega &= 0, \\ \text{res}_{d_4} \omega &= 0, & \text{res}_{d_5} \omega &= kdy, & \text{res}_{d_6} \omega &= k \frac{v_6}{4} dv_6. \end{aligned}$$

- (ii) *For the standard root variable normalization  $\mathcal{X}(\delta) = a_0 + a_1 + a_2 = 1$  we need to take  $k = -1$  and root variables  $a_i$  are then given by*

$$a_0 = 1 - \lambda, \quad a_1 = -n, \quad a_2 = n + \lambda. \quad (3.9)$$

*Proof.* For comprehensive examples of such calculations, refer to [DT18, DFS20], here, we only explain one example. Consider the root  $\alpha_0$  and represent it as a difference of two effective classes,

$$\begin{aligned} \alpha_0 &= 2\mathcal{H}_x + 2\mathcal{H}_y - \mathcal{F}_1 - 2\mathcal{F}_3 - \mathcal{F}_4 - \mathcal{F}_5 - \mathcal{F}_6 - \mathcal{F}_7 - \mathcal{F}_8 \\ &= [2H_x + 2H_y - F_1 - F_3 - F_4 - F_5 - F_6 - F_7 - F_8] - [F_3]. \end{aligned}$$

The first class is a class of a proper transform of a  $(2, 2)$ -curve passing through points  $q_1, q_3, \dots, q_8$ . A direct computation reveals that its equation in the affine  $(x, y)$  chart is  $c_1(y - n) + x(c_2 + c_1y(t - 2x(y + \lambda - 1))) = 0$ , where  $c_1$  and  $c_2$  are parameters. The second class corresponds to the exceptional divisor  $F_3$ . Subsequently, we utilize the irreducible component  $d_1$ , leading to

$$(H_x - F_2 - F_3) \bullet (2H_x + 2H_y - F_1 - F_3 - F_4 - F_5 - F_6 - F_7 - F_8) = (H_x - F_2 - F_3) \bullet F_3 = 1,$$

so we need to consider these curves in the  $(X, y)$ -chart. In this chart, the proper transform  $2H_x + 2H_y - F_{1345678}$  intersects  $d_1$  at  $(X = 0, 1-\lambda)$ , while the exceptional divisor  $F_3$  intersects  $d_1$  at the point  $q_3(X = 0, 0)$ . Computing the symplectic form  $\omega$  in the  $(X, y)$ -chart,

$$\omega = k \frac{dx \wedge dy}{x} = -k \frac{dX \wedge dy}{X},$$

we see that

$$\text{res}_{d_1} \omega = \text{res}_{X=0} -k \frac{dX \wedge dy}{X} = -kdy, \quad a_0 = \mathcal{X}(\alpha_0) = \int_0^{1-\lambda} -kdy = k(\lambda - 1).$$

Similarly, we obtain

$$a_0 = k(\lambda - 1), \quad a_1 = kn, \quad a_2 = -k(n + \lambda).$$

Imposing the normalization condition  $\mathcal{X}(\delta) = a_0 + a_1 + a_2 = -k = 1$ , we find that  $k = -1$ .

*Remark 10.* Note that the root variable evolution under the discrete step  $n \rightarrow n + 1$  is given by

$$\bar{a}_0 = a_0, \quad \bar{a}_1 = a_1 - 1, \quad \bar{a}_2 = a_2 + 1,$$

which corresponds to the standard translation on the root basis given by (2.12). □

### 3.8 The Change of Coordinates

We are now ready to prove Theorem 1, which is the main result of the paper.

*Proof. (Theorem 1)* This computation is standard, with detailed examples available in [DT18, DFS20], so we only provide a brief outline here. From the change of basis in Lemma 8 on the Picard lattice for the coordinate classes,

$$\mathcal{H}_x = \mathcal{H}_q + \mathcal{H}_p - \mathcal{E}_3 - \mathcal{E}_4, \quad \mathcal{H}_y = \mathcal{H}_q + \mathcal{H}_p - \mathcal{E}_1 - \mathcal{E}_3,$$

we see that  $x$  and  $y$  are projective coordinates on pencils of  $(1, 1)$ -curves in the  $(q, p)$ -coordinates, and  $x$  corresponds to the pencil passing through  $p_3$  and  $p_4$ , while  $y$  corresponds to the pencil passing through  $p_1$ ,  $p_3$ . Thus, we take the change of coordinates to be

$$x(q, p) = \frac{A(qp - a_1) + Bq}{C(qp - a_1) + Dq}, \quad y(q, p) = \frac{Kqp + L}{Mqp + N},$$

where the coefficients  $A, \dots, N$  are still to be determined. For example, the correspondence  $H_p - E_3 - E_5 = F_4 - F_5$  means that

$$(x, Y)(q, P = 0) = \left( \frac{Aq + Bq \cdot 0 - Aa_1 \cdot 0}{Cq + Dq \cdot 0 - Ca_1 \cdot 0}, \frac{N \cdot 0 + Mq}{L \cdot 0 + Kq} \right) = \left( \frac{A}{C}, \frac{M}{K} \right) = (0, 0), \quad \text{and so } A = M = 0,$$

then we can take  $B = N = 1$  to get

$$x(q, p) = \frac{q}{C(qp - a_1) + Dq}, \quad y(q, p) = Kqp + L.$$

The correspondence  $E_1 - E_2 = H_x - F_2 - F_3$  means that  $X(Q = 0, 0) = D = 0$ , thus,

$$x(q, p) = \frac{q}{C(qp - a_1)}.$$

Proceeding in the same way, from the correspondence  $E_6 - E_7 = F_6 - F_7$  we deduce that  $C^2 = 2K$ , from the correspondence  $E_4 = H_y - F_3$  we get  $L = -\frac{a_1 C^2}{2}$ . Thus, we get

$$y(q, p) = \frac{C^2}{2}(qp - a_1).$$

Finally, from the correspondence  $E_7 - E_8 = F_7 - F_8$  we get  $Ct = -s$ , from the correspondence  $E_8 = F_8$  and (1.8), we obtain that  $C = -\sqrt{2}$ . The inverse change of variables can now be either obtained directly, or computed in the similar way. This concludes the proof of Theorem 1. □

## Acknowledgements

We express our sincere thanks to Prof. A. Dzhamay for his enthusiastic help and valuable discussions.

M. Zhu acknowledges the support of the National Natural Science Foundation of China under Grant No. 12201333, the Natural Science Foundation of Shandong Province (Grant No. ZR2021QA034), and the Breeding Plan of Shandong Provincial Qingchuang Research Team (Grant No. 2023KJ135).

## References

- [BVA10] L. Boelen and W. Van Assche, *Discrete Painlevé equations for recurrence coefficients of semi-classical Laguerre polynomials*, Proc. Amer. Math. Soc. **138** (2010) 1317-1331.
- [CI10] Y. Chen and A. Its, *Painlevé III and a singular linear statistics in Hermitian random matrix ensembles, I*, J. Approx. Theory **162** (2010) 270-297.
- [CJ14] P. A. Clarkson and K. Jordaan, *The relationship between semiclassical Laguerre polynomials and the fourth Painlevé equation*, Constr. Approx. **39** (2014) 223-254.
- [CJK16] P. A. Clarkson, K. Jordaan and A. Kelil, *A generalized Freud weight*, Stud. Appl. Math. **136** (2016) 288-320.
- [DFS20] A. Dzhamay, G. Filipuk and A. Stokes, *Recurrence coefficients for discrete orthogonal polynomials with hypergeometric weight and discrete Painlevé equations*, J. Phys. A: Math. Theor. **53** (2020) 495201.
- [DFS22] A. Dzhamay, G. Filipuk and A. Stokes, *Differential equations for the recurrence coefficients of semiclassical orthogonal polynomials and their relation to the Painlevé equations via the geometric approach*, Stud. Appl. Math. **148** (2022) 1656-1702.
- [DT18] A. Dzhamay and T. Takenawa, *On some applications of Sakai's geometric theory of discrete Painlevé equations*, SIGMA Symmetry Integrability Geom. Methods Appl. **14** (2018), Paper No. 075, 20.
- [FVAZ12] G. Filipuk, W. Van Assche and L. Zhang, *The recurrence coefficients of semi-classical Laguerre polynomials and the fourth Painlevé equation*, J. Phys. A: Math. Theor. **45** (2012) 205201.
- [GR14] B. Grammaticos and A. Ramani, *Discrete Painlevé equations: an integrability paradigm*, Phys. Scr. **89** (2014) 038002.
- [KNY17] K. Kajiwara, M. Noumi and Y. Yamada, *Geometric aspects of Painlevé equations*, J. Phys. A: Math. Theor. **50** (2017) 073001.
- [Kac90] V. G. Kac, *Infinite-dimensional Lie algebras*, 3rd ed., Cambridge University Press, 1990.
- [Mag95] A. P. Magnus, *Painlevé-type differential equations for the recurrence coefficients of semi-classical orthogonal polynomials*, J. Comput. Appl. Math. **57** (1995) 215-237.
- [Sak01] H. Sakai, *Rational surfaces associated with affine root systems and geometry of the Painlevé equations*, Comm. Math. Phys. **220** (2001) 165–229.
- [Sak07] H. Sakai, *Problem: discrete Painlevé equations and their Lax forms*, Algebraic, analytic and geometric aspects of complex differential equations and their deformations. Painlevé hierarchies, RIMS Kôkyûroku Bessatsu, B2, Res. Inst. Math. Sci. (RIMS), Kyoto, 2007, pp. 195–208.
- [Sha13] I. R. Shafarevich, *Basic algebraic geometry 1*, Third ed., Springer, Heidelberg, 2013, Varieties in projective space.

- [TD25] E. Trunina and A. Dzhamay, *Orthogonal Polynomials for the Gaussian Weight with a Jump and Discrete Painlevé Equations*, Proceedings of OPSFA, 2025 (preprint).
- [VA18] W. Van Assche, *Orthogonal polynomials and Painlevé equations*, Australian Mathematical Society Lecture Series, vol. 27, Cambridge University Press, Cambridge, 2018.